Inorganic Chemistry

ARTICLE

pubs.acs.org/IC

Ligand Binding Intermediates of Nitrosylated Human Hemoglobin Induced at Low Temperature by X-ray Irradiation

Alessandro Arcovito*,† and Stefano Della Longa*,‡

†Istituto di Biochimica e Biochimica Clinica, Università Cattolica del Sacro Cuore, Largo F. Vito 1,00168, Roma, Italy

‡Dipartimento di Medicina Sperimentale, Università dell' Aquila via Vetoio, loc. Coppito II 67100 L'Aquila, Italy

ABSTRACT: Under prolonged X-ray irradiation, the ferrous heme of nitrosylated human adult hemoglobin derivative (HbNO) undergoes a reversible transition generating a 5-coordinate species, due to release of the Fe-NO bond. The overall process can be investigated using X-ray absorption near edge structure (XANES) spectroscopy. In this work, Fe K-edge XANES spectra were measured at $T < 15$ K, pH 9.2, i.e., on a high-affinity state (R-HbNO) where all the hemes are 6-coordinate, and at pH 6.5 in the presence of inositol hexakis-phosphate (IHP), i.e., on a low-affinity ligated state (T-HbNO) where the iron-hemes of the α-chains are 5-coordinate due to breaking of the Fe-proximal histidine bond. Under X-ray irradiation, 5-coordinate Fe-hemes are populated in both R-HbNO and T-HbNO, the Fe-NO bond lysis induced in T-HbNO involving rebinding of the proximal histidine to the transiently populated 4-coordinate hemes of the α-chains. A detailed analysis of the spectra confirms that different intermediate states in the ligand binding cooperative process of hemoglobin can be populated by X-ray irradiation, and that the part of the energy associated to the R-T quaternary transition, that is transmitted to the heme site, can be monitored by XANES spectroscopy.

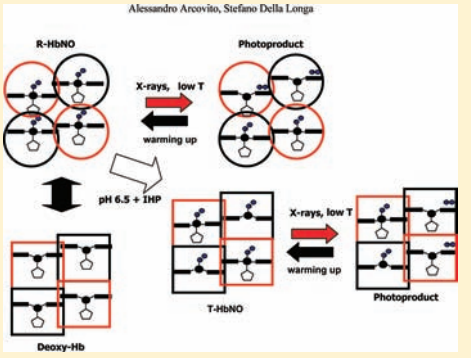

INTRODUCTION

Most of our knowledge about the atomic structure of proteins and other biologically relevant molecules is derived from X-ray studies, which at present are mainly performed by using high brilliant synchrotron facilities, and, hopefully in the near future, will be carried out by means of ultrahigh brilliant XFEL sources, allowing us to link structural data to ultrafast dynamics, using either X-ray diffraction[1] or X-ray absorption spectroscopy (XAS).[2,3] As an example, flash photolysis of hemoglobin derivatives (O_2, NO, CO) in the femtosecond time scale has revealed that two short-lived species, Hb I* and Hb II*, are formed on the absorption of a visible photon by the heme.[4] The lifetime of Hb II* is 2.5 ps (before fast recombination), and this species is significantly populated when the ligand is NO or O_2, but not when the ligand is CO. Thus, the apparently low quantum yield of photodissociation for the former two ligands could be in part explained by the fast recombination of the ligand from the highly reactive state Hb II*, a physiologically relevant information. However, the understanding of such biochemical events will not be complete without solving molecular structures along the reaction path from the initially photoexcited Franck−Condon state to a thermally equilibrated excited state. Under this perspective, it seems important to demonstrate the capacity to extract both the kinetics and the structure of intermediate states by spectroscopic techniques like XAS.

Several side effects[5] are known to follow the primary interaction (radiolysis) between X-rays and the water solvent surrounding the proteins both in crystalline and solution state. Among them, the cleavage of specific bonds has been reported, and in some cases it has been deliberately provoked by investigators interested in using X- or γ-rays to trigger protein dynamics events.[6−11]

In a previous work,[12] we showed that X-rays can be used to both induce and probe, by X-ray absorption near edge structure (XANES) spectroscopy, the Fe-CO bond lysis in carbonmonoxy-myoglobin (MbCO) at very low temperature. We have observed a long lasting CO dissociation process at $T < 15$ K, and the subsequent CO recombination process by increasing temperature, as well as in classical photolysis experiments,[13,14] without using any external source of visible light. Our experiment showed that this effect can be deliberately used allowing alternative sample conditions and experimental setup requirements for X-ray studies of hemeprotein ligand binding by means of synchrotron radiation. Novel X-ray experiments can be planned, aimed at a dynamical characterization of those 5-coordinate ferrous states in heme containing protein that are the species involved in binding external ligands. In the present work we report an extension of our previous findings to human nitrosylhemoglobin (HbNO).

Nitric oxide was considered nonphysiological but a useful molecule as a probe of structure−function relationships up to the 1980s when it was discovered to activate cell signaling pathways via the membrane hemeprotein guanylate cyclase, by (according to the proposed model[15]) an NO-dependent breaking of the Fe-proximal His bond. Moreover, a possible functional role of HbNO in human and mammalian mechanisms was proposed, involving NO

Received: May 23, 2011
Published: August 30, 2011

depletion[16] or nitrite reductase activity[17,18] by deoxy-hemoglobin, that should be able in the latter case to reduce naturally occurring nitrite (NO_2) to the vasoactive NO molecule; thus, the interest in NO as a physiologically relevant ligand of Hb has greatly increased.

The electronic structure of NO, i.e., of the NO^- ion in the ionic binding model, is similar to O_2, resulting in a bent arrangement as exogenous ligand of the ferrous ion of heme containing proteins. Relative to O_2, the NO^- ion donates more electron density, which is mostly directed onto the iron d_{z^2} orbital, increasing competition with the charge donated by the trans ligand (the proximal histidine in our case); i.e., the two trans ligands bind in an anticooperative way. This is the basic mechanism proposed[15] as underlying the physiological role of NO in the cell signaling pathway involving guanylate cyclase: the presence of NO in the tissue would be able to "cut off" the Fe-proximal histidine bond, triggering in turn a structural rearrangement of the heme-based NO sensor, thus inducing the activation of the enzymatic production of cyclic guanylyl monophosphate (cGMP) and the subsequent cellular response.

An anticooperative trans ligand binding is partly inducible in HbNO: indeed the interaction of NO to the T-quaternary state of ferrous deoxy-hemoglobin (deoxy-Hb), obtained in conditions when the T→R transition is inhibited, is accompanied by the weakening or partial breaking of the Fe-proximal histidine bonds,[19] whereas when using O_2, CO, etc., this effect does not occur.[20] The X-ray structure[19] of crystals of deoxy-Hb exposed to gaseous NO under a variety of conditions shows that the binding of NO favors breaking of the Fe-proximal histidine bonds of the α-subunits but not of the β-subunits, giving a heterogeneous $\alpha_2\beta_2$ tetramer with two 5-coordinate NO bound-hemes (α-chains) and two 6-coordinate NO bound-hemes (β-chains).

Low-temperature photolysis protocols are classical procedures aimed to trap intermediate states of the ligand binding process in myoglobin, hemoglobin, and related hemeproteins for structural studies.[21−25] In these experimental conditions the ligand cannot escape from the hydrophobic pocket containing the heme center, and according to the chosen protocol of illumination and/or temperature dependence, the local rearrangement of the heme site associated to internal ligand migration in a given tertiary or quaternary state of the protein can be probed. In the present work, we show that the X-ray induced lysis of Fe-exogenous ligand bond is common in hemeproteins, and demonstrate that the simple "pump−probe" XANES spectroscopy procedure can be applied, at low temperature, in order to study intermediate states of HbNO in two extreme cases: the R-state at pH 9.2, and a ligated T-state, which is obtained by adding inositol exakisphosphate (IHP), a heterotropic, allosteric effector able to induce the R→T transition in hemoglobin,[26] at pH 6.5. The comparison between the XAS spectra of the unligated R-state and the unligated T-state, accumulated by X-rays pumping, and frozen at low temperature, gives clues on the constraints to the heme rearrangement following NO release, due to the quaternary state. Hence, these experiments may contribute to clarifying structural aspects of the reaction mechanism of hemoglobin with NO, and more in general of hemeproteins with their ligands.

METHODS

Human hemoglobin was prepared according to a standard procedure,[27] from fresh blood. Ferrous R-HbNO was obtained with the Antonini−Brunori method[28] at a 3 mM final concentration, pH 9.2, borate 2% in NaOH, 20% glycerol, by adding, in a nitrogen atmosphere, 100 mM sodium dithionite; the color changed to grape-red (deoxy-Hb), and successively sodium nitrite was added anaerobically to a final concentration of 30 mM. The final adduct displayed the characteristic cherry-red color of HbNO. A large excess of dithionite is necessary to both scavenge oxygen and drive the reaction between dithionite and nitrite and the subsequent formation of the nitrosyl adduct. Similarly, ferrous T-HbNO was prepared as 3 mM, pH 6.5, in buffer Bis-Tris 0.1 M, 20% glycerol, 30 mM IHP. The molar ratio of [effector]/[Hb] of 10 used here is of the same order as that used in NMR and EPR experiments working at near millimolar concentration of Hb.[26,29] Immediately after preparation, samples were loaded in the sample holder, frozen in liquid nitrogen, and then transferred into the cryostat, where the temperature was set to 120 K for the optical alignment of the beamline.

Glycerol is a widely used cryoprotectant in crystallographic and optical studies[30] owing to its ability to increase the homogeneity of the sample, being able to form transparent glasses when cryocooled, so that 10−20% glycerol solution is normally used in low-temperature XAS measurements. Moreover, glycerol has been widely discussed as a radical scavenger.[31] The influence of glycerol on the R-T equilibrium and dynamics of hemoglobin is known: the 20% volume/volume glycerol concentration used in this work corresponds to less than 3 M concentration. According to Bulone et al.[32] this glycerol concentration produces a $\Delta\log P_{50} = +0.15$ in the oxygen affinity curve of hemoglobin at pH 7. In any case the cosolvent effect seems far lower than the effect produced by considering only the pH difference ($\Delta\log P_{50}$ about −0.9 between pH 6.5 and pH 9) and is negligible by considering the further effect induced by IHP.[26] As far as it concerns dynamics, the cosolvent induced viscosity certainly affects the bimolecular phase of recombination, but to our knowledge no relevant effect exists on the geminate phase (confined in the heme hydrophobic pocket), which occurs at very low temperature; actually the time-resolved kinetic curves of CO geminate recombination to hemoglobin, measured at room temperature at 0% and 75% glycerol concentration, were found to be indistinguishable.[33]

X-ray absorption measurements have been collected in fluorescence mode at ESRF-BM30B, Grenoble, by using a 30-elements ultrapure Ge detector and a Si(220) double crystal monochromator. The sample was maintained in an open cycle liquid helium cryostat. The sample was in a helium atmosphere, the temperature of the sample holder being monitored by a platinum/carbon resistor with 0.1° accuracy. The spectra were calibrated by assigning the first inflection point of the Fe foil spectrum to 7112 eV. The energy stability of each spectrum was carefully assessed by checking the position of a glitch in the I_0 at 7220 eV.

The concentration of the samples and the protocols of X-ray irradiation for R- and T- HbNO were identical within the reproducibility of the experimental conditions (in the same experimental session and with identical optical setup of the beamline). Alignment of the beam on each sample was done at $T = 120$ K. Then, the temperature was lowered at 6 K and the time zero of irradiation at this temperature coincides with the first point of the first XAS spectrum collected. The entire experimental hutch of the synchrotron beamline was in the dark during the experimental runs. Saturation of the X-ray induced effects was obtained for both R-HbNO and T-HbNO. The absorbed X-ray dose D (Gy) was calculated according to Owen et al.[5,12,31,34] to be about $D = 600$ Gy per second. As the time window necessary to reach steady state conditions in our X-ray irradiation protocols was about 600 min for T-HbNO (14 spectra) and 800 min for R-HbNO (17 spectra), a value of 22 and 28 MGy, respectively, was evaluated, which is still below the maximum recommended dose to a protein crystal of 30 MGy.[5] The overall protocol adopted is similar to that previously described for MbCO.[12] As we are aware, at $T < 100$K, no radical produced in the external solvent can enter the hydrophobic pocket. Only a thermalized electron can reach the metal center leading to the well-known photoreduction concerns affecting ferric hemeproteins,[31,34] and inducing release of the exogenous ligand in ferrous hemeproteins. The energy position of the XANES edge is an extremely

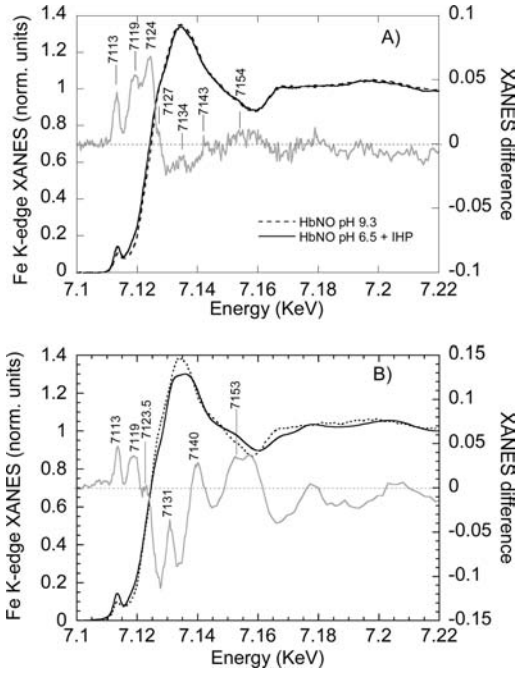

Figure 1. (A) XANES spectra of HbNO at pH 9.2 (dotted line) and at pH 6.5 + IHP (solid line). Their difference spectrum is also reported (gray line). (B) Reference spectra for 6-coordinate (i.e., MbNO, dotted line) and 5-coordinate (i.e., TPP-NO, solid line) NO adducts of the heme. The energy scale is in keV, while the energy of the features is in eV.

sensitive probe of the iron charge and the irreversible photoreduction effects occurring at the ferric hemeproteins,[10] as well as of the presence or not of the exogenous ligand in the ferrous derivatives. In fact, as previously published in the case of MbCO,[12] for which the experiment was dedicated to fully characterize it, an X-rays induced lysis of the CO molecule was observed at $T < 15$ K and the process was fully reversible as the starting spectrum was recovered after increasing temperature. The same effect has also been observed in MbNO and HbNO (data not published): the spectral changes at the end of the irradiation protocol at 6 K are reversible, and the starting XANES spectrum displays again all the features of the fully ligated NO-adduct after increasing temperature to $T = 100$ K. Thus, no damage occurs at the heme site level. Moreover, as mentioned above, the evaluated absorbed dose in our experiments is below the maximum recommended dose of 30 MGy to a cryocooled crystal (containing 30−70% of water, at $T = 77$ K) in protein crystallography. Under this maximum value a typical protein crystal is considered to maintain an ordered three-dimensional arrangement good enough for giving a high resolution diffraction pattern.[5] Actually, a combined cryo-XRD (at 1.4 Å resolution) and XAS experiment on the same single crystal of cyanomet-myoglobin was perfomed[35] demonstrating that the protein maintained both the same local structure and the same long-range arrangement for the overall irradiation time. Thus, we believe that, even in the case of ferrous HbNO, at the temperature of our experiment, not only the hydrophobic pocket but also the whole protein matrix remains frozen in its original tertiary and quaternary arrangement, residual effects from radical ions being limited to the near environment of the trapped solvent molecules and the peripheral sites of the protein.

RESULTS

The Fe K-edge XANES spectra of both R-HbNO and T-HbNO show evolution under prolonged X-ray irradiation at $T < 15$ K, reverting to the initial spectra by increasing temperature to $T > 100$ K. We have interpreted these changes as due to

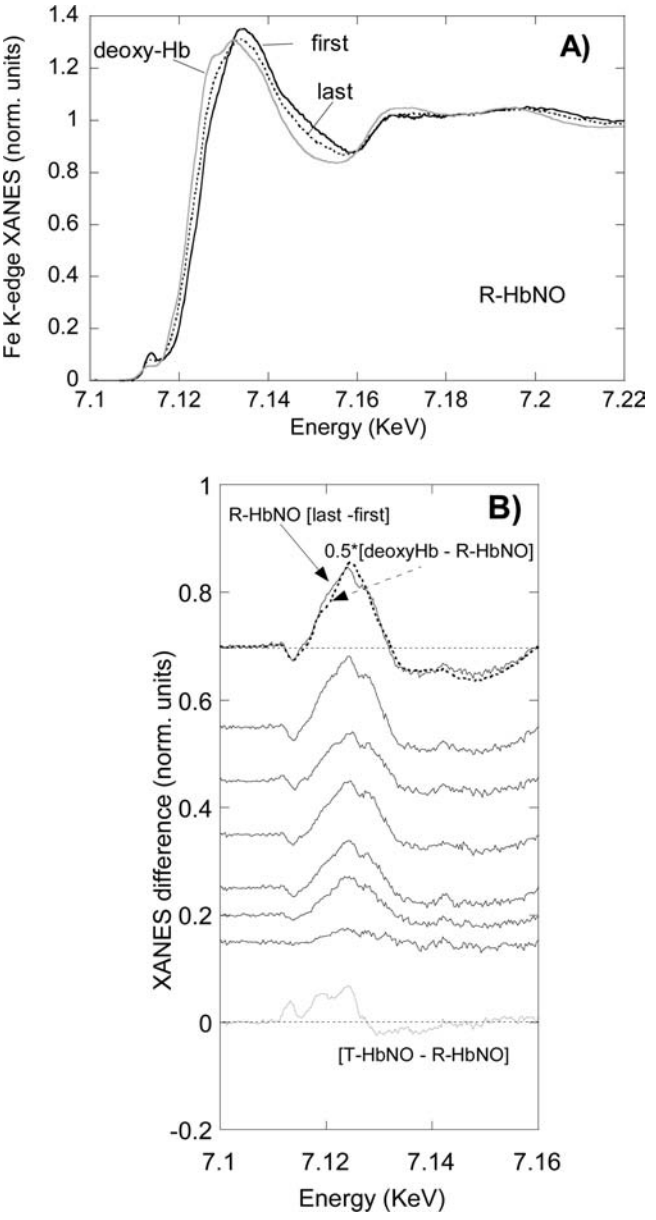

Figure 2. (A) XANES spectra of R-HbNO under X-rays: first spectrum (solid line), at steady state under irradiation after 800 min (dotted line) and deoxy-Hb (gray line). (B) From bottom to top: XANES difference spectra [T-HbNO − R-HbNO ($t = 0$)], and R-HbNO (t) − R-HbNO ($t = 0$) for $t = 100$, 220, 290, 360, 490, 610, and 800 min. The last difference spectrum (at top, solid line) is superimposed onto that of [deoxy-Hb − R-HbNO ($t = 0$)] multiplied by 0.5.

X-ray induced release of NO in a fractional population of heme sites. In the following (Figures 1−4) a detailed description of the experiments is done, while in Figure 5 a sketch representing the heme tetramers inside R- and T-HbNO, populated during our protocols, should be helpful to clarify the experiments done and their interpretation.

The XANES spectra of HbNO at pH 9.2 (R-ligated state, dotted line) and at pH 6.5 in the presence of IHP (T-ligated state, solid line) are reported in Figure 1A, together with the T-R XANES difference spectrum. The difference spectrum displays positive peaks at the pre-edge (7113 eV), at the rising edge (7119 and 7124 eV), and in the low energy region (7127, 7134, 7143,

dx.doi.org/10.1021/ic201086u |Inorg. Chem. 2011, 50, 9423–9429

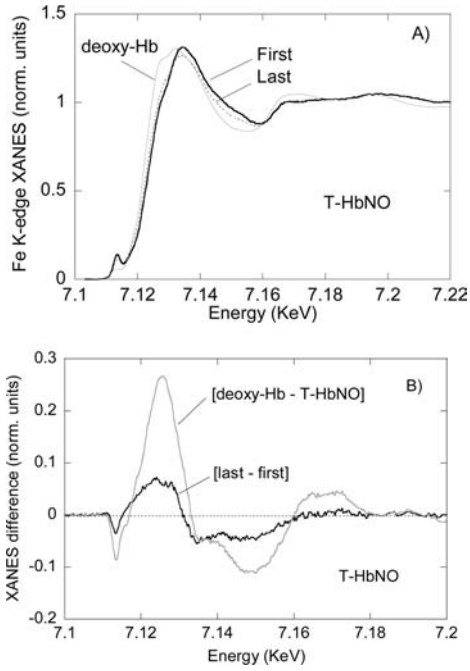

Figure 3. (A) XANES spectra of T-HbNO under X-rays: first spectrum (solid line), at steady state under irradiation after 600 min (dotted line) and deoxy-Hb (gray line). (B) XANES difference spectra: T-HbNO [last − first] and [deoxy-Hb − T-HbNO].

and 7154 eV). The presence of 5-coordinate NO-hemes, due to rupture of the Fe-His bonds in the α-chains, whose percentage depends on pH, have been previously determined in T-HbNO by extensive EPR investigations,[29] as indicated by the appearance of the characteristic triplet hyperfine structure (A_z = 17 G at g_z = 2.009) of the 5-coordinate nitrosyl heme model system. According to the amplitude of this feature, a fraction of 0.8−0.9 of 5-coordinate α-nitrosyl-hemes has been calculated at pH 6.5 in the presence of IHP. Therefore, the spectra of Figure 1A are compared with spectra of opportune model systems in Figure 1B, i.e., the 5-coordinate Fe(II)-tetraphenyl-porphyrin-NO (TPP-NO) and the nitrosyl-myoglobin (MbNO) bearing a 6-coordinate Fe-heme. The spectra in Figure 1A could be expected to represent linear combinations of those in Figure 1B, even though subtle differences may be present, due to the different environment of the metal in the model compounds used. Indeed, the difference spectra of Figure 1A,B are not identical, because of the contributions of far atoms that are different in the model system with respect to HbNO, and because in the T-R difference spectrum, the contributions from 6-coordinate hemes of T-ligated HbNO β-chains are still present. However, the similarity between the two spectra confirms that the difference spectrum of Figure 1A contains the XANES fingerprints for the rupture of the Fe-proximal histidine bond in the α-chains of T-HbNO.

Evidence that the XANES difference spectrum can be used to distinguish between 5-coordinate NO-hemes and 5-coordinate deoxy-like hemes is given by experiments of X-ray induced lysis of the Fe-6th ligand bond at low temperature: The XANES spectra of R-HbNO (pH 9.2) and T-HbNO (pH 6.5 + IHP) evolve under prolonged X-ray irradiation at T < 15 K as shown in Figures 2 and 3. The first spectrum of R-HbNO (solid line), the last spectrum acquired after about 800 min (dotted line), and the spectrum of deoxy-Hb (gray line) are superimposed in Figure 2A.

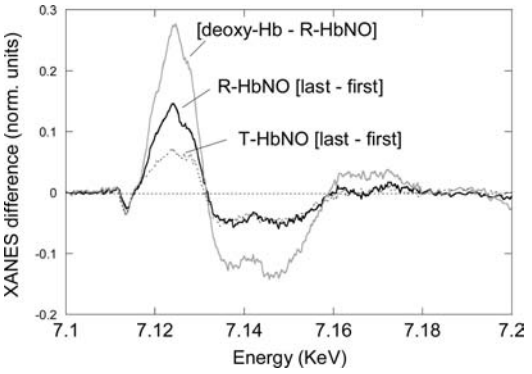

Figure 4. XANES difference spectra: solid line R-HbNO [last − first], dotted line T-HbNO [last − first]; gray line [deoxy-Hb − R-HbNO].

In Figure 2B, the XANES difference spectrum [T-HbNO − R-HbNO] is reported again, at bottom. Moreover, in the same frame, the progression of the XANES difference spectra [R-HbNO-(t) − R-HbNO(first)] under X-rays is shown after 100, 220, 290, 380, 490, 610, and 800 min. The last difference spectrum is well superimposed onto that of [deoxy-Hb − R-HbNO(first)] multiplied by 0.5, thus suggesting the formation of 5-coordinate Fe-hemes due to the release of the NO molecule in about 50% of the heme sites. The experimental data shown in Figure 2B demonstrate that the XANES fingerprint due to dynamic events in which 5-coordinate species are formed by the rupture of the Fe-proximal ligand bond are quite different from those formed by rupture of the Fe-distal ligand bond. We note that this effect is easily distinguishable even if both the proximal and distal first ligands are nitrogen atoms, and both events involve only a partial population of the hemes in Hb.

The same experimental protocol has been repeated for T-HbNO and reported in Figure 3A. Again, the spectra of T-HbNO (first spectrum, dotted line), T-HbNO (last spectrum, after 600 min, gray line), and deoxy-Hb (solid line) are displayed. In Figure 3B the spectral difference [T-HbNO(last) − T-HbNO-(first)] is compared with the difference [deoxy-Hb − T-HbNO-(first)]. The two difference spectra are now not superimposable (in particular, the isosbestic points of the process, the zeroes of the difference spectra at about 7115 and 7130 eV, are different), and we explain this result according to the following interpretation: X-rays induce in T-HbNO the rupture of the Fe-NO bond, but a percentage of α-hemes remains still 5-coordinate with NO. It is important to note that the presence of 4-coordinate Fe-heme due simply to the rupture of the Fe-NO bond in the 5-coordinate α-nitrosyl hemes is ruled out by the complete absence of a prominent $1s \rightarrow 4p_z$ transition at 7117 eV which is assigned as a typical feature of square planar, 4-coordinate hemes.[36] Therefore, the XANES spectrum of T-HbNO under X-ray contains contributions from two kinds of 5-coordinate hemes, i.e., the first NO-ligated, and the other deoxy-like: the difference spectra [T-HbNO-(last) − T-HbNO(first)] and [deoxy-Hb − T-HbNO(first)] do not superimpose because of the contributions from those 5-coordinate NO-ligated hemes not affected by X-rays that are hidden in the [T-HbNO(last) − T-HbNO(first)] but are present in the [deoxy-Hb − T-HbNO(first)] spectrum.

This interpretation led us to compare directly the two X-ray photolysis experiments, summarized in the two difference spectra shown in Figures 2B and 3B, that for clarity we will name now as R-spectrum and T-spectrum, with the standard difference

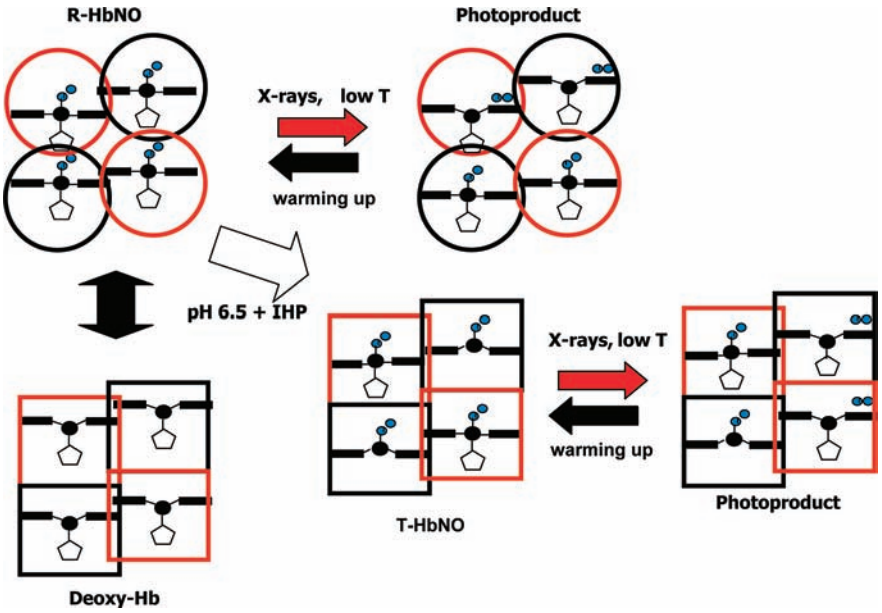

Figure 5. Scheme of the ligand binding states of the $\alpha_2\beta_2$ tetramer of HbNO investigated in the present work. α-Subunits are depicted in black, β-subunits in red. According to our interpretation, NO dissociates from both α-hemes and β-hemes in T-HbNO; in the α-chains, fast reassociation of the proximal histidine to the highly reacting 4-coordinate heme occurs, so that only 5-coordinate deoxy-like hemes accumulate under X-ray pumping.

between T-deoxyHb − R-HbNO, that we will refer to as the T-R-spectrum. This comparison will allow us to know if XANES is able to distinguish between ligand dissociation processes carried out within the R- or T-quaternary state, and that one carried out along the R-T transition; the results could be important for time-resolved investigation of hemoglobin at room temperature carried out by XAS.

In Figure 4, the R-spectrum, the T-spectrum and the T-R-spectrum are compared. The spectra exhibit the same isosbestic points, confirming that the same overall process is occurring. The magnitude of the T-R spectrum, calculated around the main peak at 7124 eV is approximately 2 times that of the R-spectrum, and 4 times that of the T-spectrum; however, the same evaluation done at about 7145 eV gives 2-times for both the R- and T- spectra. In principle, the T-spectrum and the R-spectrum may be different not only for the fraction of deoxy-like, 5-coordinate states obtained from the X-ray photolysis, but also for the contributions of NO bound 5-coordinated hemes involved in the dissociation process of T-HbNO, and for the degree of structural/electronic relaxation at the heme site. However, the R-spectrum and T-spectrum are indeed superimposable, apart from the rising edge region around 7125 eV; thus, our interpretation is that the number of 5-coordinate deoxy-like states created after X-ray induced photolysis of NO is comparable, so that a large fraction of NO bound 5-coordinate hemes has been converted via the lysis induced by X-rays to a deoxy-like species, thus involving fast rebinding of the proximal histidine (this point will be addressed in detail in the Discussion section). However, the remaining amplitude in the R-spectrum, with respect to the T-spectrum, is presumably due to a lower structural relaxation that is accomplished by the T-ligated state when the exogenous ligand is removed. This last sentence is indeed supported by the available X-ray structures[19] of HbNO, i.e., that of R2-S-nitroso-HbNO and T-HbNO, pointing out a partial Fe-heme displacement in T-HbNO with respect to R2-S-nitroso-HbNO (having an in-plane iron), i.e., a greater similarity to the Fe-heme structure of deoxy-Hb.

DISCUSSION

Prolonged exposition to X-rays produces breaking of the Fe-NO bond in HbNO, as well as in other derivatives of Mb and Hb and other globins. Besides MbCO[12] and carbonmonoxy-neuroglobin[37] (NgbCO, a globin found in neurons of the vertebrates) the same effect has occasionally been observed, with different magnitude, working at 15 K with heme-containing *H. ducreyi* Cu, Zn carbonmonoxy-superoxyde dismutase,[38] and with numerous mutants of MbCO and NgbCO, with MbNO, and carbonmonoxy-cytochrome P450 (data not shown). However, the effect was not observed, or negligible, at least in one case, i.e., in truncated HbCO from *Thermobifida fusca*. This recombinant protein is characterized by a higher amplitude of the geminate phase at room temperature with respect to the other mentioned proteins (A. Boffi, personal communication). Reasonably, a kinetic equilibrium exists between the X-ray pumped dissociation rate and the geminate recombination rate at low temperature, as well as in standard photolysis experiments. Thus, the effect could be hidden in *T. fusca* because geminate recombination overwhelms dissociation even at very low temperature. Several parameters like the brilliance of the X-ray source used, the X-ray "photolysis quantum yield", the Fe-heme net charge, and the polarity of the near environment should be investigated to check their capacity to affect this equilibrium.

Turning back to human HbNO in our experimental conditions, according to Figure 5, our study has allowed us to compare the heme structures in the ligated R-state (R-HbNO) and the unligated T-state (deoxy-Hb), with that of a ligated T-state (T-HbNO), as well as, via X-ray lysis, to some specific intermediates such as a partially ligated R-state and a partially ligated T-state. In the present paper, discussion is focused on experimental evidence of the X-ray photolysis effect; however, a quantification of

both the fractional populations, and the structural relaxation, could be attempted by fitting these R- and T-spectra with a linear combination of coordination model systems, or by using the software package MXAN[39] in order to extract the geometry, and will be the topic of future work.

In T-HbNO an apparent fraction of about 0.5 photolyzed hemes is obtained in the absence of any signature associated with 4-coordinate hemes. This evidence would apparently suggest that, under X-ray irradiation, NO release occurs only in the β-chains, and α-nitrosyl-Hb is produced. This derivative, frequently observed upon reaction of deoxy-Hb with limited quantities of NO, has been well characterized.[29] However, according to UV−vis low-temperature photolysis and EPR experiments reported in the literature,[40] the characteristic hyperfine structures of 5-coordinate NO-heme decrease under illumination in T-HbNO. Hence, NO from both α and β chains is supposed to participate to the photolysis process in T-HbNO as well as in R-HbNO. The apparent discrepancy between our data and EPR results can be explained, according to the huge body of knowledge derived from classical low-temperature photolysis experiments on myoglobin:[41−43] According to the photolysis protocol, under prolonged illumination the steady state accumulates along many ligand dissociation−reassociation cycles. Under photon pumping the exogenous ligand rebinding barrier increases as associated to both ligand migration and structural relaxation of the iron position with respect to the heme plane. The same process should occur in HbNO under prolonged X-ray irradiation at low temperature. Moreover, in T-HbNO it is expected that rebinding of the proximal histidine to the highly reactive 4-coordinate iron (transiently produced by NO release in the α chains) is favored, in agreement with the anticooperative model of NO binding. The recombination of proximal histidine to the iron is a diffusion-independent, unimolecular reaction, that should be fast even at very low temperature. Thus, our results are consistent with previous EPR studies by assuming unspecific NO release from both the α and β chains, followed by fast recombination of the proximal histidine to the heme irons of the α-chains. This picture could be validated in the future by time-resolved XAS experiment, if it is able to capture the fast transient 4-coordinate species.

At present, as stated in the Results section, we assume that the fraction of 5-coordinate states created after photolysis, measured by the overall amplitude of the difference spectrum, is comparable in the R- and T-states, and that the degree of structural relaxation following the rupture of the Fe-NO bond, measured by the amplitude of the feature at about 7125 eV in the R-spectrum and in the T-spectrum, is higher in the R-state than in the T-state; the Fe-heme structure in the quaternary constrained T-state, during the X-ray induced photolysis process, undergoes a lower rearrangement, as is expected for a more tense structure. Thus, our experiment shows that the part of the energy associated to the R-T quaternary transition, that is transmitted to the heme site, could be directly monitored by XANES spectroscopy.

Due to the relaxation effects discussed above, we actually cannot rule out the hypothesis that, within the heme environment, the unligated R-state structure would revert at least in part to the unligated T-state structure. However, even if only qualitatively, spectral differences between the T-spectrum and the R-spectrum of Figure 4 are still observed and can be interpreted as due to a different degree of structural distortion. Quantitative analysis still demands future time-resolved XAS experiments at room temperature, allowing us to solve the unrelaxed Fe-heme structure of the unligated R-state.

In conclusion, our paper, focused on the finding of X-ray induced photolysis, also shows the potential of XANES to reveal, and to distinguish between, intermediate states of hemoglobin. Even if our experimental conditions are far from physiological, the results give a glimpse for the interpretation of future time-resolved XAS investigations, done by pump−probe experiments using synchrotron or X-FEL sources, that could be done at room temperature,[39,44,45] being able to discern protein dynamics events related to an heterogeneous system of multiple heme subunits.

AUTHOR INFORMATION

Corresponding Authors

*E-mail: alessandro.arcovito@rm.unicatt.it (A.A.); dlonga@caspur.it (S.D.L.).

ACKNOWLEDGMENT

Authors are grateful to Prof. Bruno Giardina of the Università Cattolica del Sacro Cuore for fruitful discussions and suggestions. Financial support by the Italian Ministry of University and Research [Linea D1 "ex-60%" 2009−2010 Università Cattolica del Sacro Cuore] is acknowledged. Thanks are due to the European Synchrotron Radiation Facility (ESRF-Grenoble) for providing facilities supplies and the staff of BM30B for the helpful support.

REFERENCES

(1) Chapman, H. N.; Fromme, P.; Barty, A.; White, T. A.; Kirian, R. A.; Aquila, A.; Hunter, M. S.; Schulz, J.; DePonte, D. P.; Weierstall, U.; Doak, R. B.; Maia, F. R.; Martin, A. V.; Schlichting, I.; Lomb, L.; Coppola, N.; Shoeman, R. L.; Epp, S. W.; Hartmann, R.; Rolles, D.; Rudenko, A.; Foucar, L.; Kimmel, N.; Weidenspointner, G.; Holl, P.; Liang, M.; Barthelmess, M.; Caleman, C.; Boutet, S.; Bogan, M. J.; Krzywinski, J.; Bostedt, C.; Bajt, S.; Gumprecht, L.; Rudek, B.; Erk, B.; Schmidt, C.; Hömke, A.; Reich, C.; Pietschner, D.; Strüder, L.; Hauser, G.; Gorke, H.; Ullrich, J.; Herrmann, S.; Schaller, G.; Schopper, F.; Soltau, H.; Kühnel, K. U.; Messerschmidt, M.; Bozek, J. D.; Hau-Riege, S. P.; Frank, M.; Hampton, C. Y.; Sierra, R. G.; Starodub, D.; Williams, G. J.; Hajdu, J.; Timneanu, N.; Seibert, M. M.; Andreasson, J.; Rocker, A.; Jönsson, O.; Svenda, M.; Stern, S.; Nass, K.; Andritschke, R.; Schröter, C. D.; Krasniqi, F.; Bott, M.; Schmidt, K. E.; Wang, X.; Grotjohann, I.; Holton, J. M.; Barends, T. R.; Neutze, R.; Marchesini, S.; Fromme, R.; Schorb, S.; Rupp, D.; Adolph, M.; Gorkhover, T.; Andersson, I.; Hirsemann, H.; Potdevin, G.; Graafsma, H.; Nilsson, B.; Spence, J. C. Femtosecond X-ray protein nanocrystallography, *Nature* **2011**, *470*, 73–7.

(2) Patterson, B. D.; Abela, R. *Phys. Chem. Chem. Phys.* 2010, *12*, 5647–52.

(3) Bressler, C.; Chergui, M. *Annu. Rev. Phys. Chem.* **2010**, *61*, 263–82.

(4) Martin, J. L.; Vos, M. H. *Methods Enzymol.* **1994**, *232*, 416–30.

(5) Owen, R. L.; Rudino-Pinera, E.; Garman, E. F. *Proc. Natl. Acad. Sci. U.S.A.* **2006**, *103*, 4912–7.

(6) Schlichting, I.; Berendzen, J.; Chu, K.; Stock, A. M.; Maves, S. A.; Benson, D. E.; Sweet, R. M.; Ringe, D.; Petsko, G. A.; Sligar, S. G. *Science* **2000**, *287*, 1615–1622.

(7) Prusakov, V. E.; Steyer, J.; Parak, F. *Biophys. J.* **1995**, *68*, 2524–2530.

(8) Parak, F.; Prusakov, V. E. *Hyperfine Interact.* **1994**, *91*, 885–890.

(9) Lamb, D. C.; Arcovito, A.; Nienhaus, K.; Minkow, O.; Draghi, F.; Brunori, M.; Nienhaus, G. U. *Biophys. Chem.* **2004**, *109*, 41–58.

(10) Della Longa, S.; Arcovito, A.; Benfatto, M.; Congiu-Castellano, A.; Girasole, M.; Hazemann, J. L.; Lo Bosco, A. *Biophys. J.* **2003**, *85*, 549–58.

(11) Davydov, R.; Kappl, R.; Hüttermann, J.; Peterson, J. A. *FEBS Lett.* **1991**, *295*, 113.
(12) Della Longa, S.; Arcovito, A. *Inorg. Chem.* **2010**, *49*, 9958–61.
(13) Austin, R. H.; Beeson, K. W.; Eisenstein, L.; Frauenfelder, H.; Gunsalus, I. C. *Biochemistry* **1975**, *14*, 5355–73.
(14) Arcovito, A.; Lamb, D. C.; Nienhaus, G. U.; Hazemann, J. L.; Benfatto, M.; Della Longa, S. *Biophys. J.* **2005**, *88*, 2954–64.
(15) Traylor, T. G.; Sharma, V. S. *J. Am. Chem. Soc.* **1992**, *31*, 2847–2848.
(16) Eich, R. F.; Li, T.; Lemon, D. D.; Doherty, D. H.; Curry, S. R.; Aitken, J. F.; Mathews, A. J.; Johnson, K. A.; Smith, R. D.; Phillips, G. N., Jr.; Olson, J. S. *Biochemistry* **1996**, *35*, 6976–83.
(17) Cosby, K.; Partovi, K. S.; Crawford, J. H.; Patel, R. P.; Reiter, C. D.; Martyr, S.; Yang, B. K.; Waclawiw, M. A.; Zalos, G.; Xu, X.; Huang, K. T.; Shields, H.; Kim-Shapiro, D. B.; Schechter, A. N.; Cannon, R. O., 3rd; Gladwin, M. T. *Nat. Med.* **2003**, *9*, 1498–505.
(18) Jensen, F. B. *J. Exp. Biol.* **2009**, *212*, 3387–93.
(19) Chan, N. L.; Kavanaugh, J. S.; Rogers, P. H.; Arnone, A. *Biochemistry* **2004**, *43*, 118–32.
(20) Paoli, M.; Liddington, R.; Tame, J.; Wilkinson, A.; Dodson, G. *J. Mol. Biol.* **1996**, *256*, 775–92.
(21) Alben, J. O.; Beece, D.; Bowne, S. F.; Eisenstein, L.; Frauenfelder, H.; Good, D.; Marden, M. C.; Moh, P. P.; Reinisch, L.; Reynolds, A. H.; Yue, K. T. *Phys. Rev. Lett.* **1980**, *44*, 1157–1160.
(22) Powers, L.; Sessler, J. L.; Woolery, G. L.; Chance, B. *Biochemistry* **1984**, *23*, 5519–23.
(23) Chance, B.; Fischetti, R.; Powers, L. *Biochemistry* **1983**, *22*, 3820–9.
(24) Schlichting, I.; Berendzen, J.; Phillips, G. N. J.; Sweet, R. M. *Nature* **1994**, *371*, 808–812.
(25) Teng, T. Y.; Srajer, V.; Moffat, K. *Nat. Struct. Biol.* **1994**, *1*, 701–5.
(26) Yonetani, T.; Park, S. I.; Tsuneshige, A.; Imai, K.; Kanaori, K. *J. Biol. Chem.* **2002**, *277*, 34508–20.
(27) Rossi-Fanelli, A.; Antonini, E.; Caputo, A. *J. Biol. Chem.* **1961**, *236*, 391–6.
(28) Antonini, E.; Brunori, M. *Hemoglobin and Myoglobin in their Reactions with Ligands*; North-Holland: Amsterdam, 1971.
(29) Yonetani, T.; Tsuneshige, A.; Zhou, Y.; Chen, X. *J. Biol. Chem.* **1998**, *273*, 20323–33.
(30) Beitlich, T.; Kuhnel, K.; Schulze-Briese, C.; Shoeman, R. L.; Schlichting, I. *J. Synchrotron Radiat.* **2007**, *14*, 11–23.
(31) O'Neill, P.; Stevens, D. L.; Garman, E. F. *J. Synchrotron Radiat.* **2002**, *9*, 329–32.
(32) Bulone, D.; Cupane, A.; Cordone, L. *Biopolymers* **1983**, *22*, 119–23.
(33) Huang, J.; Ridsdale, A.; Wang, J.; Friedman, J. M. *Biochemistry* **1997**, *36*, 14353–65.
(34) Corbett, M. C.; Latimer, M. J.; Poulos, T. L.; Sevrioukova, I. F.; Hodgson, K. O.; Hedman, B. *Acta Crystallogr., Sect. D: Biol. Crystallogr.* **2007**, *63*, 951–60.
(35) Arcovito, A.; Benfatto, M.; Cianci, M.; Hasnain, S. S.; Nienhaus, K.; Nienhaus, G. U.; Savino, C.; Strange, R. W.; Vallone, B.; Della Longa, S. *Proc. Natl. Acad. Sci. U.S.A.* **2007**, *104*, 6211–6.
(36) Della Longa, S.; Arcovito, A.; Brunori, M.; Castiglione, N.; Cutruzzolà, F.; D'Angelo, P.; Giardina, G.; Rinaldo, S. *J. Phys.: Conf. Ser.* **2009**, *190*, 012202.
(37) Arcovito, A.; Moschetti, T.; D'Angelo, P.; Mancini, G.; Vallone, B.; Brunori, M.; Della Longa, S. *Arch. Biochem. Biophys.* **2008**, *475*, 7–13.
(38) D'Angelo, P.; Zitolo, A.; Pacello, F.; Mancini, G.; Proux, O.; Hazemann, J. L.; Desideri, A.; Battistoni, A. *Arch. Biochem. Biophys.* **2010**, *498*, 43–9.
(39) Della-Longa, S.; Chen, L. X.; Frank, P.; Hayakawa, K.; Hatada, K.; Benfatto, M. *Inorg. Chem.* **2009**, *48*, 3934–42.
(40) el-Jaick, L. J.; Wajnberg, E.; Linhares, M. P. *Int. J. Biol. Macromol.* **1991**, *13*, 289–94.
(41) Nienhaus, G. U.; Mourant, J. R.; Chu, K.; Frauenfelder, H. *Biochemistry* **1994**, *33*, 13413–30.
(42) Lamb, D. C.; Nienhaus, K.; Arcovito, A.; Draghi, F.; Miele, A. E.; Brunori, M.; Nienhaus, G. U. *J. Biol. Chem.* **2002**, *277*, 11636–44.
(43) Chu, K.; Ernst, R. M.; Frauenfelder, H.; Mourant, J. R.; Nienhaus, G. U.; Philipp, R. *Phys. Rev. Lett.* **1995**, *74*, 2607–2610.
(44) Chergui, M. *ChemPhysChem* **2002**, *3*, 713–8.
(45) Chen, L. X.; Zhang, X.; Lockard, J. V.; Stickrath, A. B.; Attenkofer, K.; Jennings, G.; Liu, D. J. *Acta Crystallogr., Sect. A* **2010**, *66*, 240–51.